Vertically aligned ZnO nanostructures grown on graphene layers

Yong-Jin Kim, Jae-Hyun Lee, and Gyu-Chul Yi

Citation: Applied Physics Letters **95**, 213101 (2009); doi: 10.1063/1.3266836
View online: http://dx.doi.org/10.1063/1.3266836
View Table of Contents: http://scitation.aip.org/content/aip/journal/apl/95/21?ver=pdfcov
Published by the AIP Publishing

Vertically aligned ZnO nanostructures grown on graphene layers

Yong-Jin Kim[1]
[1]*Department of Materials Science and Engineering, National Creative Research Initiative Center for Semiconductor Nanorods, POSTECH, Pohang, Gyeongbuk 790-784, Republic of Korea*

Jae-Hyun Lee[2] and Gyu-Chul Yi[2,a)]
[2]*Department of Physics and Astronomy, National Creative Research Initiative Center for Semiconductor Nanorods, Seoul National University, Seoul 151-747, Republic of Korea*

(Received 30 September 2009; accepted 30 October 2009; published online 24 November 2009)

We report the vertical growth of ZnO nanostructures on graphene layers and their photoluminescence (PL) characteristics. ZnO nanostructures were grown vertically on the graphene layers using catalyst-free metal-organic vapor-phase epitaxy. The surface morphology of the ZnO nanostructures on the graphene layers depended strongly on the growth temperature. Further, interesting growth behavior leading to the formation of aligned ZnO nanoneedles in a row and vertically aligned nanowalls was also observed and explained in terms of enhanced nucleation on graphene step edges and kinks. Additionally, the optical characteristics and carbon incorporation into ZnO were investigated using variable-temperature PL spectroscopy. © *2009 American Institute of Physics*. [doi:10.1063/1.3266836]

Graphene-based hybrid nanostructures with inorganic nanomaterials provide a link between solid-state nanostructures and two-dimensional molecular science. The growth of semiconductor nanocrystals on graphene layers is particularly interesting because nanostructures, such as nanoneedles and nanowalls, can offer additional functionality to graphene in advanced electronics and optoelectronics. Graphene has a great potential for novel electronic devices based on "quasirelativistic" transport behavior due to its remarkable electrical and thermal properties including a carrier mobility exceeding 10^4 $cm^2/V\,s$ and a thermal conductivity of 10^3 $W/m\,K$.[1–4] Meanwhile, semiconductor nanoneedles grown on graphene layers are good candidates for field emission emitters due to their sharp tips, high aspect ratio, and high thermal and mechanical stability.[5,6] Semiconductor nanowalls that have an extremely large surface-to-volume ratio and high porosity can also be exploited in novel electrical devices, including sensitive biological and chemical sensors and efficient energy conversion and storage devices.[7–9] Accordingly, with the excellent electrical and thermal characteristics of graphene layers, growing semiconductor nanostructures on graphene layers would enable their novel physical properties to be exploited in diverse sophisticated device applications. This letter introduces the metal-organic vapor-phase epitaxial growth of ZnO nanoneedles and nanowalls on graphene layers.

ZnO nanostructures were grown on few-layer-graphene (FLG) sheets using catalyst-free metal-organic vapor-phase epitaxy (MOVPE). Before growing the ZnO nanostructures, FLG sheets were transferred onto the SiO_2/Si substrates using a simple mechanical exfoliation technique.[10] Micro-Raman spectroscopy confirmed the successful preparation of the graphene layers and was used to determine the number of graphene layers.[11] After preparing the graphene layers, ZnO nanostructures were grown using MOVPE with the reactants diethylzinc (DEZn) and oxygen. For preventing the oxidation of graphene layer, we introduced DEZn flow into the reactor before flowing oxygen. The details of ZnO nanostructure growth using MOVPE are reported elsewhere.[6]

The optical qualities of the as-grown ZnO nanostructures on the graphene layers were investigated using photoluminescence (PL) spectroscopy. The PL was measured at 17–200 K using a closed-cycle refrigeration system. Details of the PL measurements are described elsewhere.[12]

The density and dimensions of the ZnO nanostructures changed dramatically upon using FLG sheets as the growth seed layer. As shown in Fig. 1, the morphology of the ZnO nanostructures on the graphene layers was very different from that in the region of the SiO_2/Si substrate that was not covered by the graphene layer. Straight ZnO nanoneedles grew on the graphene layers with good vertical alignment,

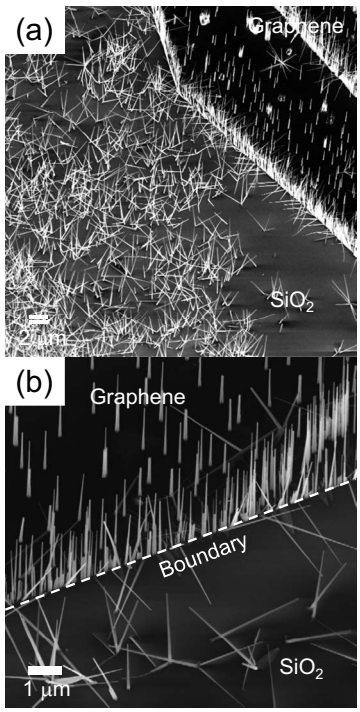

FIG. 1. FE-SEM image of ZnO nanostructures grown on the graphene layers transferred onto the SiO_2/Si substrates.

a)Author to whom correspondence should be addressed. Electronic addresses: gcyi@snu.ac.kr and gyuchul.yi@gmail.com.

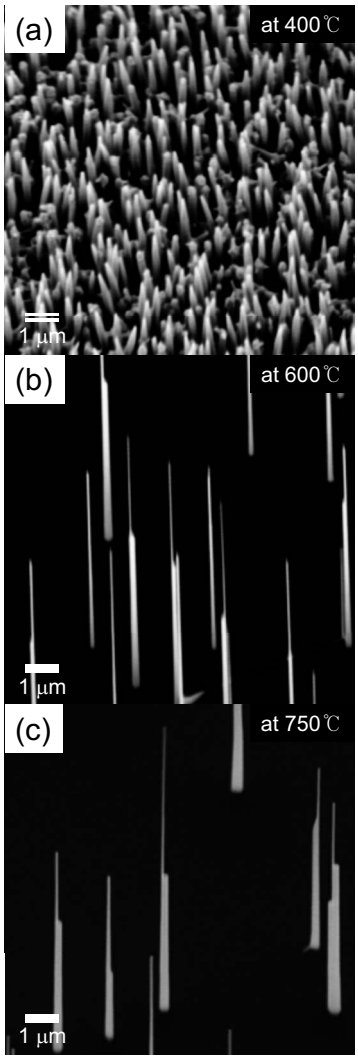

FIG. 2. FE-SEM images of ZnO nanostructures grown on the graphene layers at (a) 400, (b) 600, and (c) 750 °C.

while entangled ZnO nanowires with poor vertical alignment grew on the SiO_2/Si substrate. The ZnO nanoneedles grown on the graphene layers at 750 °C for 1 h had a typical density of 5×10^7 cm^{-2} and a length of 3.5 ± 0.5 μm, while ZnO nanoneedles grown on the SiO_2/Si substrate under identical growth conditions had a higher density of 5×10^8 cm^{-2} and a longer mean length of 5.5 ± 0.8 μm. The low density and short lengths of the ZnO nanoneedles on the graphene layers resulted from the reduced ZnO nucleation on the graphene layers presumably due to the large lattice constant misfit between ZnO and graphene. Meanwhile, the ZnO nanostructure growth behavior at the boundaries of graphene layers was very interesting. As shown in Fig. 1(b), very dense ZnO nanoneedles grew along the boundaries and even became connected with each other at their bottoms to form nanowalls. The enhanced growth of ZnO nanostructures were previously observed upon growing ZnO nanowalls on the GaN substrates with a SiO_2 mask layer. This behavior strongly suggests that the nucleation and growth of the ZnO nanoneedles were more active along the boundaries.

The surface morphology of the ZnO nanostructures on the graphene layers depended strongly on the growth temperature. Figure 2 shows field emission scanning electron microscopy (FE-SEM) images of ZnO nanostructures grown vertically on graphene layers transferred to the SiO_2/Si substrates at 400, 600, and 750 °C for 1 h. At the lower growth temperature of 400 °C, the ZnO nanostructures had a mean length of 1.0 ± 0.1 μm and a diameter of 100 ± 10 nm. The nanostructure density was 4×10^9 cm^{-2}, which is comparable to those grown on single-crystalline Si and sapphire substrates or 1×10^{10} cm^{-2}.[6,13] By contrast, ZnO nanostructures grown at the higher temperature of 600 °C were tapered and had sharp tips, forming nanoneedle. The mean diameter and length were 90 ± 20 nm and 4.0 ± 0.6 μm, respectively. The nanoneedle density decreased to 8×10^7 cm^{-2} due to the decreased nucleation rate with increasing growth temperature. ZnO nanoneedles grown at 750 °C had a morphology similar to those grown at 600 °C, but the nanoneedle density decreased to 5×10^7 cm^{-2}. These results indicate that higher growth temperature generally yielded a lower density of ZnO nanoneedles on the graphene layers presumably due to a reduction in the ZnO nucleation rate. It is also noted that ZnO nanostructures grown at higher temperatures typically exhibit a higher aspect ratio (longer length and smaller diameter) and a shaper tip. Surface diffusion length of the adsorbed atoms on the sidewalls of ZnO nanostructures may increase with growth temperature, and adsorbed atoms can easily move to the nanostructure tips, resulting in the formation of ZnO nanoneedles with an increased aspect ratio.

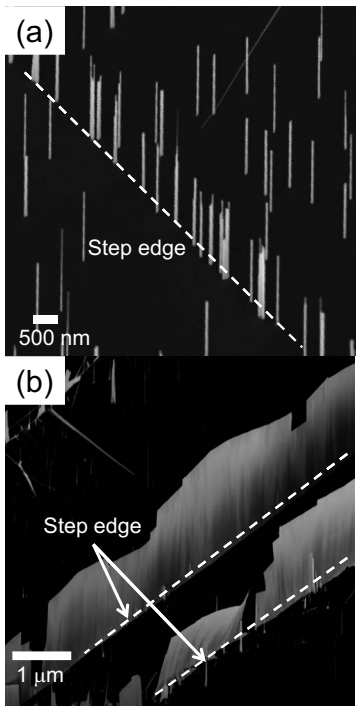

FIG. 3. FE-SEM images of ZnO nanostructures near the step edges of graphene [(a) and (b)].

The interesting surface morphologies of the ZnO nanostructures grown on the graphene layers were further observed. As shown in Fig. 3(a), ZnO nanoneedles were generally located randomly, but some of them were aligned in a row, as indicated by a dotted line. In addition to ZnO nanoneedles, vertically aligned nanowalls were also formed, as depicted in Fig. 3(b). This growth behavior may be explaned in terms of the enhanced growth on step edges of graphene layers, which were formed during the process of transferring graphene layers from graphite onto a substrate. The step edges may serve as nucleation centers for nanoneedle growth

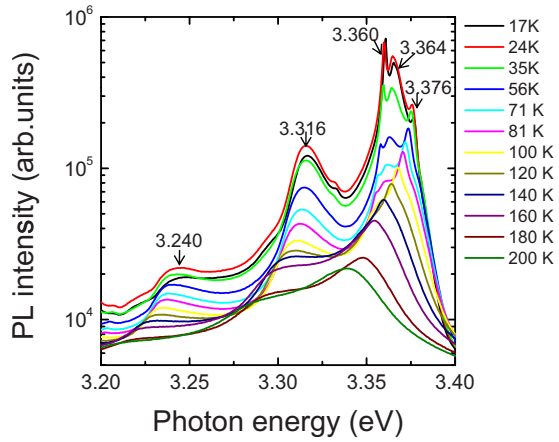

FIG. 4. (Color online) Temperature-dependent PL spectra of ZnO nanostructures grown on the graphene layers.

because nucleation and crystal growth on a step edge are favored over nucleation and growth on a terrace. Nucleation and crystal growth are further enhanced at a kink in the step edge. Hence, step edges with a high density of kinks may induce the formation of aligned nanoneedles. Moreover, if there are many kinks in a graphene step edge, the high density of ZnO nanoneedles could form a nanowall along the step edge. The enhanced nucleation of ZnO at the step edges of graphene layers may offer a way to control the position of ZnO nanostructures on graphene layers if the graphene step edges are formed artificially in a controlled manner.

The optical characteristics of the ZnO nanostructures were investigated using variable-temperature PL spectroscopy. Figure 4 shows a series of PL spectra of ZnO nanostructures deposited on the graphene layers, which were measured at temperatures of 17–200 K. The PL spectrum at 17 K typically shows five distinct near-band-edge (NBE) emission peaks at 3.376, 3.364, 3.360, 3.316, and 3.240 eV with full width at half maximum (FWHM) values of 2–13 meV. The strong, sharp NBE emission indicates the high optical quality of the ZnO nanostructures on the graphene layers. Compared with the reported PL peak positions for ZnO nanostructures, thin films, and bulk crystals, the dominant PL peaks observed at 3.360 and 3.364 eV are tentatively attributed to neutral-donor bound exciton peaks, and the PL peak at 3.376 to a free exciton peak (X_A).[12,14–16] From the PL spectra, no additional exciton peak associated with carbon impurities in carbon-doped ZnO films[17] was observed at 3.356 eV. This suggests that carbon atoms in graphene were not incorporated into the ZnO nanoneedles during their growth. The PL characteristics of ZnO nanostructures on graphene layers were almost the same to those of ZnO nanostructures on single-crystalline substrates.[6,13] The observation of the free exciton peak, neutral-donor bound exciton peaks, and weak deep level emission related to defects indicates high optical quality of ZnO nanoneedles grown on the graphene layers. The temperature-dependent behavior of the NBE PL peaks confirms the origins of the tentatively assigned excitonic emission peaks.[12] The excellent optical properties may originate from the high crystallinity of ZnO nanoneedles since stacking faults or dislocations were not observed from the transmission electron microscopy (TEM) images of ZnO nanoneedles grown on graphene layers (data not shown here).

The ability to grow high-quality ZnO nanostructures on the graphene layers should greatly increase the versatility and power of these building blocks for nanoscale photonic and electronic device applications. By combining the excellent thermal and electrical characteristics of graphene and the optical characteristics of ZnO nanostructures, the graphene-ZnO hybrid nanostructures may be exploited in high-performance optoelectronic device applications. From the perspective of device applications, obtaining such high-purity ZnO nanostructures on graphene is a significant advance toward device fabrication because the precise control of conductivity via simple impurity *in situ* doping, ion implantation, or diffusion should be easy.

In conclusion, ZnO nanostructures were grown vertically on the graphene layers using a catalyst-free MOVPE method. The aspect ratio and density of the nanostructures depended strongly on the growth temperature. Furthermore, interesting growth behavior, the formation of aligned ZnO nanoneedles in rows and vertically aligned nanowalls, was observed, presumably resulting from the enhanced nucleation at graphene step edges. Additionally, PL spectra of the ZnO nanostructures on the graphene layers included a free exciton PL peak with no carbon-related defect peak, suggesting that high-quality ZnO nanostructures were grown on the graphene layers without deterioration of the graphene layers during MOVPE.

This work was supported financially by the National Creative Research Initiative Project (Grant No. R16-2004-004-01001-0) of the Korea Science and Engineering Foundation (KOSEF).

[1] K. S. Novoselov, A. K. Geim, S. V. Morozov, D. Jiang, M. I. Katsnelson, I. V. Grigorieva, S. V. Dubonos, and A. A. Firsov, Nature (London) **438**, 197 (2005).
[2] Y. B. Zhang, Y. W. Tan, H. L. Stormer, and P. Kim, Nature (London) **438**, 201 (2005).
[3] A. A. Balandin, S. Ghosh, W. Z. Bao, I. Calizo, D. Teweldebrhan, F. Miao, and C. N. Lau, Nano Lett. **8**, 902 (2008).
[4] K. S. Kim, Y. Zhao, H. Jang, S. Y. Lee, J. M. Kim, J. H. Ahn, P. Kim, J. Y. Choi, and B. H. Hong, Nature (London) **457**, 706 (2009).
[5] C. J. Lee, T. J. Lee, S. C. Lyu, Y. Zhang, H. Ruh, and H. J. Lee, Appl. Phys. Lett. **81**, 3648 (2002).
[6] W. I. Park, G.-C. Yi, M. Y. Kim, and S. J. Pennycook, Adv. Mater. (Weinheim, Ger.) **14**, 1841 (2002).
[7] S. W. Kim, H. K. Park, M. S. Yi, N. M. Park, J. H. Park, S. H. Kim, S. L. Maeng, C. J. Choi, and S. E. Moon, Appl. Phys. Lett. **90**, 033107 (2007).
[8] E. Hosono, S. Fujihara, I. Honna, and H. S. Zhou, Adv. Mater. (Weinheim, Ger.) **17**, 2091 (2005).
[9] X. D. Wang, Y. Ding, Z. Li, J. H. Song, and Z. L. Wang, J. Phys. Chem. C **113**, 1791 (2009).
[10] K. S. Novoselov, A. K. Geim, S. V. Morozov, D. Jiang, Y. Zhang, S. V. Dubonos, I. V. Grigorieva, and A. A. Firsov, Science **306**, 666 (2004).
[11] D. Yoon, H. Moon, Y. W. Son, G. Samsonidze, B. H. Park, J. B. Kim, Y. Lee, and H. Cheong, Nano Lett. **8**, 4270 (2008).
[12] W. I. Park, Y. H. Jun, S. W. Jung, and G.-C. Yi, Appl. Phys. Lett. **82**, 964 (2003).
[13] W. I. Park, D. H. Kim, S. W. Jung, and G.-C. Yi, Appl. Phys. Lett. **80**, 4232 (2002).
[14] D. C. Reynolds, D. C. Look, B. Jogai, C. W. Litton, T. C. Collins, W. Harsch, and G. Cantwell, Phys. Rev. B **57**, 12151 (1998).
[15] T. Makino, C. H. Chia, N. T. Tuan, Y. Segawa, M. Kawasaki, A. Ohtomo, K. Tamura, and H. Koinuma, Appl. Phys. Lett. **76**, 3549 (2000).
[16] B. K. Meyer, H. Alves, D. M. Hofmann, W. Kriegseis, D. Forster, F. Bertram, J. Christen, A. Hoffmann, M. Strassburg, M. Dworzak, U. Haboeck, and A. V. Rodina, Phys. Status Solidi B **241**, 231 (2004).
[17] S. T. Tan, X. W. Sun, Z. G. Yu, P. Wu, G. Q. Lo, and D. L. Kwong, Appl. Phys. Lett. **91**, 072101 (2007).